


Metabolic engineering of crocins and picrocrocin apocarotenoids in potato group phureja

Lourdes Gómez-Gómez^{1,2} | Alberto José López-Jimenez^{1,3} | Cristian Martinez Fajardo¹ | Lucía Morote¹ | Sarah Frusciante⁴ | José Luis Rambla^{5,6} | Gianfranco Diretto⁴ | Ángela Rubio-Moraga^{1,3} | María Mondejar-López¹ | Enrique Niza^{1,2} | Javier Argandoña³ | Silvia Presa⁵ | Antonio Granell⁵ | Oussama Ahrazem^{1,3} 

¹Instituto Botánico, Universidad de Castilla-La Mancha, Albacete, Spain

²Facultad de Farmacia. Departamento de Ciencia y Tecnología Agroforestal y Genética, Universidad de Castilla-La Mancha, Albacete, Spain

³Escuela Técnica Superior de Ingeniería Agronómica y de Montes y Biotecnología. Departamento de Ciencia y Tecnología Agroforestal y Genética, Universidad de Castilla-La Mancha, Albacete, Spain

⁴Italian National Agency for New Technologies, Energy, and Sustainable Development (ENEA), Biotechnology laboratory, Casaccia Research Centre, Rome, Italy

⁵Instituto de Biología Molecular y Celular de Plantas, Consejo Superior de Investigaciones Científicas-Universidad Politécnica de València, Valencia, Spain

⁶Departamento de Biología, Bioquímica y Ciencias Naturales, Universitat Jaume I, Castellón de la Plana, Spain

Correspondence

Oussama Ahrazem, Instituto Botánico, Universidad de Castilla-La Mancha, Campus Universitario s/n, Albacete 02071, Spain.

Email: oussama.ahrazem@uclm.es

Antonio Granell, Instituto de Biología Molecular y Celular de Plantas, Consejo Superior de Investigaciones Científicas-Universidad Politécnica de València, Valencia, Spain.

Email: agranell@ibmcp.upv.es

Funding information

Ministerio de Ciencia e Innovación,

Grant/Award Numbers:

BIO2016-77000-R,

PIB2020-114761RB-I00; Junta de

Comunidades de Castilla-La Mancha,

Grant/Award Numbers:

SBPLY/17/180501/000234,

SBPLY/21/180501/000012

Abstract

The stigmas of *Crocus sativus* accumulate the exclusive apocarotenoids crocin and picrocrocin, which are dried and desiccated to make commercial saffron. In addition to providing characteristic organoleptic qualities, saffron apocarotenoids are valuable compounds in the pharmaceutical and health industries. Previously, we developed Desirée potato tubers enriched with these apocarotenoids which also showed increased potential benefits for human health. In the current study, *Solanum tuberosum* (*S. tuberosum*) Group Phureja 01H15 which accumulates high levels of zeaxanthin, was engineered to produce saffron apocarotenoids to increase the levels of these metabolites in potato tubers using a construct namely O6, which contains the *CsCCD2L*, *UGT74AD1*, and *UGT709G1* genes necessary for the biosynthesis of crocin and picrocrocin under the control of the patatin promoter. Here, we obtained transgenic *S. tuberosum* Group Phureja 01H15 lines with high concentrations of crocins and picrocrocin (up to 3.648 mg/g DW, 2.345 mg/g DW, respectively), which were up to 10 and 3 times higher than those obtained in the Desirée background, respectively. Furthermore, we performed transcriptome analyses of tubers from Desirée and 01H15 wild type and carrying O6 construct. Differentially expressed gene analysis revealed transcript changes not only on tuber carotenoid and apocarotenoid genes but also in other related pathways, suggesting a possible role in isoprenoid metabolism remodeling. Thus, this heterologous system serves as a robust platform for the production of these valuable metabolites.

KEYWORDS

carotenoid cleavage dioxygenases, crocins, picrocrocin, potato, saffron, transcriptome

This is an open access article under the terms of the [Creative Commons Attribution](https://creativecommons.org/licenses/by/4.0/) License, which permits use, distribution and reproduction in any medium, provided the original work is properly cited.

© 2024 The Author(s). *Engineering Reports* published by John Wiley & Sons Ltd.

1 | INTRODUCTION

Carotenoid compounds can be defined by a common C40 polyene backbone bearing 3 to 11 conjugated double bonds with different stereo configurations. The introduction of end-ring structures, hydroxylation, oxygenation, and other modifications lead to broad structural diversity among the more than 1200 known carotenoids.¹ The polyene structure of carotenoids, which is responsible for their role in photosynthesis, antioxidant capacity and color, makes them susceptible to oxidation, in which double bonds are cleaved to produce carbonyl products called apocarotenoids.² Virtually all living organisms can catabolize carotenoids, which can occur by either non-enzymatic and non-specific reactions such as lipoxygenase co-oxidation or photo-oxidation³ or by enzymatic oxidative degradation reactions^{4,5}; to form apocarotenoids. This latter cleavage can occur at any of the polyene double bonds, which, together with subsequent modifications, explains the structural diversity and tremendous physicochemical properties of natural apocarotenoids. In addition, some apocarotenoids can act immediately as signaling molecules, such as β -cyclocitral, while many others undergo further modifications (such as oxidations, reductions, cyclizations, methylations, glycosylations, etc.) to form active compounds with diverse biological roles and functions.⁶

The biosynthesis of apocarotenoid during plant development and stress responses is intricately linked to physiological and ecological functions such as pollinator and seed disperser attraction, plant growth promotion, pathogen defense, and herbivore resistance.⁷ Beyond growth regulation, apocarotenoids are also involved in plant defense mechanisms. Compounds such as abscisic acid (ABA), are fundamental in the plant's response to abiotic stress, including drought and salinity. ABA regulates stomatal closure to prevent water loss, thus enhancing drought tolerance. Furthermore, apocarotenoids are implicated in the defense against pathogens through the production of signaling molecules that activate plant immune responses. For example, β -ionone, has been shown to possess antimicrobial properties and can induce the expression of defense-related genes. Apocarotenoids perform important functions in the plant's interaction with its surroundings, promoting reproductive success and survival. Many apocarotenoids operate as signaling molecules, attracting helpful species and enabling pollination and seed dissemination, both of which are necessary for plant proliferation and genetic variety. Furthermore, intracellular glycosylation of several C13 apocarotenoids with hydroxyl groups seen in a number of plants, increases their solubility and decreases their toxicity.⁸ This glycosylation process regulates carotenoid homeostasis in the plant. By altering the solubility and activity of these chemicals, glycosylation assists the plant in managing and mitigating any harmful consequences, hence preserving cellular health. Furthermore, glycosylated apocarotenoids may play an important role in the plant's response to photo-oxidative stress by functioning as protective agents that shield cellular components from damage induced by prolonged light exposure.⁷

Plant apocarotenoids have a great impact on human health by preventing or alleviating chronic diseases or their symptoms. According to Li et al.,⁹ ABA is an endogenous immune regulator in animals and may be used to treat a number of human disorders. In addition, strigolactones (SL) show anti-cancer activity.¹⁰ Among volatile apocarotenoids, screening of aroma compounds revealed the cancer-preventive potential of β -ionone¹¹ and members of the damascenone group. Furthermore, apocarotenoids have garnered significant attention because of their biotechnological applications in food processing, medicines, cosmetics, fragrances, and agriculture.¹²

The specific enzymes that catalyze the oxidative cleavage of double bonds in the carotenoid polyene chain, generating apocarotenoid precursors, are known as carotenoid cleavage dioxygenases (CCDs), which also recognize and cleave apocarotenoids. CCD enzymes occur as a multigene family in fungi, plants, animals, and bacteria.² These enzymes are classified as mononuclear non-heme iron enzymes and have a stiff seven-bladed β -propeller as its basic architecture.¹³ In most cases, CCD enzymes catalyze the dioxygen (O_2)-induced cleavage of non-aromatic double bonds, producing aldehyde, dialdehyde, or ketone compounds.¹⁴ However, some CCDs are capable of catalyzing accessory reactions involving isomerizations of double bonds¹⁵ and rearrangements of the carbon backbone of carotenoids.¹⁶ The 65 kDa protein (RPE65), a member of the retinal pigment epithelium subfamily, that is essential to vertebrate visual function, is one example of a biological reaction in which oxidative cleavage is not the primary biological reaction catalyzed.¹⁷

Crocins and safranal are mainly known to be responsible for the color and aroma of saffron spice.¹⁸ In addition to their attractive color and aroma, the apocarotenoids of saffron exhibit bioactive properties that have various therapeutic and pharmacological applications. Indeed, apocarotenoids from saffron and bixa have long been known for their health-promoting properties.¹⁹

In order to overcome the limitations in obtaining saffron apocarotenoids from the original source, while considering advances in metabolic engineering and its evolution to synthetic biology, the scientific community has mobilized the biosynthetic pathway of apocarotenoids from saffron to other host organisms and searched for a cost-effective production of these rare metabolites.²⁰ Genes related to saffron that were initially involved in the biosynthesis of apocarotenoids in stigmas have been altered genetically in tomato fruits, tobacco plants, and potato tubers using different techniques. This has led to the biosynthesis and accumulation of high levels of crocin and picrocrocin in other tissues.^{21–24}

In an attempt to improve the content of the apocarotenoids crocins and picrocrocin in potato tubers, we report here the production of these metabolites in stable transgenic lines of *S. tuberosum* Group Phureja 01H15 WT, a potato tuber which accumulates high levels of the precursor zeaxanthin. This tuber is characterized by its short dormancy period, making it an excellent candidate for regions with multiple growing seasons. This cultivar is particularly noted for its high nutritional value, including elevated levels of vitamins, minerals, and high carotenoid content. The elevated levels of carotenoids contribute to the yellow-orange flesh, which is both visually appealing and nutritionally superior.²⁵ We performed this through the expression of three *Crocus* genes *CsCCD2L*, *UGT74AD1*, and *UGT709G1* engineered into Phureja under the control of the tuber-specific promoter patatin. Additionally, transcriptome analysis was performed in both wild-type and transgenic tubers 01H15 WT and the results were compared to previously transformed and wild type Desirée potato using the same construct to understand whether the introduction of the three genes affects different metabolic pathways in each background. Of interest, the results indicated that 01H15WT accumulated a higher content of crocins and picrocrocin (3.648 mg/g DW, 2.345 mg/g DW, respectively), which is up to 10-fold more than the Desirée background. Transcriptomic analyses were carried out using Desirée WT (D-WT) and Desirée-O6 (D-O6) together with 01H15WT (H-WT) and 01H15WT-O6 (H-O6). Notably, differentially expressed genes (DEGs) observed in the four samples, revealed a strong impact not only on tuber carotenoids and apocarotenoid pathways but also on other metabolic pathways, such as starch and plant hormones.

2 | METHODS

2.1 | Growth of tubers

S. tuberosum Group Phureja 01H15 WT referred hereafter as H-WT accumulating high amounts of zeaxanthin was used. H-WT plants were cultivated in 10 cm diameter pots either from seed tubers or from tissue culture plants generated in vitro. The temperature of the greenhouse, where the plants were raised, was kept at 20/15°C day and night. The mean duration of the day was 16 hours, and the maximum irradiance was approximately 10,500 mol m⁻² s⁻¹. Plants were collected for their tubers just after flowering and before senescence.

2.2 | Vector construction and producing transgenic potato plants

The same construct O6 = pDGB3α2[pPATCsCCD2LT35S-pNos-Hyg-T35S-pPATCsUGT74AD1T35S-pPATCsUGT709G1T35S-] described by²³ was mobilized to *Agrobacterium tumefaciens* (*A. tumefaciens*). The plasmid was transferred by electroporation into *A. tumefaciens* strain LBA4404 and used for stable potato transformation, as previously described.²³ Transgenic plants rooted under hygromycin selection were screened for the presence of the corresponding genes by genomic DNA PCR. To check the transgenic lines, genomic DNA was extracted from leaves using a Plant Genomic DNA Kit (www.intronbio.com). The recovered DNA was utilized as a template in a PCR experiment. The amplified bands were purified and sequenced with an automated DNA sequencer (ABI PRISM 3730xl, Perkin Elmer, Macrogen Inc., www.macrogen.com). Positive transgenic potato plants were transferred to soil and planted in the greenhouse. All primers used to produce the final construct are listed in Supplemental Table S1.

2.3 | Analyses of carotenoid and apocarotenoid

50 mg and 10 mg of freeze-dried whole tuber samples were used to extract polar and non-polar metabolites, respectively. These samples were obtained from a pooled collection of three tubers from three separate plants to ensure a

representative and comprehensive analysis. For polar metabolite analyses, tissue samples were extracted in cold 50% MeOH. HPLC-DAD and HPLC-ESI-HRMS were used to analyze the soluble fractions, as previously reported.²⁶ Non-polar fractions were extracted with 1:1:2 cold extraction solutions (MeOH:Tris:CHCl₃) and analyzed by HPLC-APCI-HRMS and HPLC-DAD as reported before.²¹ By comparing each peak's UV spectrum with a standard, if available, and using literature data and m/z-accurate masses as provided in the PubChem database (<http://pubchem.ncbi.nlm.nih.gov/>) for the identification of monoisotopic masses, or with the Metabolomics Fiehn Lab Mass Spectrometry Adduct Calculator (<http://fiehnlab.ucdavis.edu/staff/kind/Metabolomics/MS-Adduct-Calculator/>) when adduct detection is involved, metabolites were identified by co-migration with standards. Pigments were measured by integrating peak areas, and as previously reported, these were converted to concentrations by comparison with standards.²⁷

2.4 | Analysis of volatiles

Volatile compounds were collected by headspace solid-phase microextraction (HS-SPME) and analyzed by gas chromatography coupled with mass spectrometry (GC/MS) (48). Frozen potato tubers were crushed in a cryogenic mill. A 15 mL glass vial containing 500 mg of the pulverized material was incubated in a water bath for 10 min at 30°C. Next, 2 mL of CaCl₂ 5 M and 200 µL of a pH 7.5 EDTA 500 mM solution were added and carefully stirred. The next step was to transfer 2 mL of the produced paste to a 10 mL headspace screw cap vial with a silicone/PTFE septum. Using a 65 µm PDMS/DVB solid phase microextraction fiber (SUPELCO), the volatile compounds were captured from the headspace. A CombiPAL autosampler was used to automatically extract volatiles (CTC Analytics). The vials were incubated for 10 minutes at 50°C and 500 rpm agitation. The fiber was then left under the same temperature and agitation settings for 20 minutes in the vial headspace. Desorption was carried out at 250°C for 1 minute in splitless mode in the gas chromatograph (Agilent Technologies) 6890 N injection port. Following desorption, the fiber was purified for 5 minutes at 250°C under helium flow in an SPME fiber conditioning station (CTC Analytics). Chromatography was carried out using helium as the carrier gas and a steady flow rate of 1.2 mL/min on a DB-5 ms (60 m, 0.25 mm, 1.00 µm) capillary column (J&W). The temperatures of the MS source and the GC interface were 230 and 260°C, respectively. The oven was programmed to run at 40°C for 2 minutes, ramp up to 250°C at a rate of 5°C per minute, and then hold that temperature for 5 minutes. Agilent Technologies' 5975B mass spectrometer recorded data in the following range from 35 to 250 m/z at 6.2 scans/s with electronic impact ionization at 70 eV. Chromatograms were analyzed using the MassHunter Workstation v10.1 software (Agilent Technologies).

2.5 | Samples RNA extraction, library preparation and sequencing

TRIzol reagent was used to extract total RNA from Desirée WT, transgenic Desirée, H-WT control, and H-O6-1 (Invitrogen, Carlsbad, USA). Each sample was sent to MacroGen Inc. (Seoul, South Korea; www.macrogen.com) for sequencing on an Illumina HiSeq 2000 sequencer and library building using the TruSeq Stranded RNA Sample Prep kit (San Diego, USA) at an average of 10–15 µg total RNA.

2.6 | Data processing, transcriptome assembly and annotation

RNA-seq raw read quality was assessed using FastQC.²⁸ In order to avoid biases in analysis, adaptor sequencing artifacts and low quality fragments were subsequently removed using Trimmomatic.²⁹ Trimmed reads were merged into a file to proceed with de novo assembly using Trinity with standard parameters.³⁰ Assembled contigs were further processed by CD-HIT-EST³¹ in order to cluster non-redundant transcripts, producing unique transcripts defined as “unigenes.” ORF prediction of unigenes was assessed by TransDecoder software, and annotation was performed through searches against NCBI Nucleotide (NT), NCBI Non-redundant Protein (NR), Pfam, Gene ontology (GO), UniProt and EggNOG databases using BLASTN of NCBI BLAST and BLASTX of DIAMOND software. The abundance of unigenes across samples was estimated as read counts using an RSEM algorithm.

2.7 | Analysis of differentially expressed unigenes of WT and O6 from Desirée and 01H15

DEG analysis between backgrounds was performed using Fold Change, exact test using Bioconductor Package edgeR³² per comparison pair after filtering of low expressed transcripts and TMM Normalization. The significant results were selected based on $|fc| \geq 2$ & exactTest raw p -value < 0.05 .

The count matrix for all sequenced samples was utilized to generate a Euclidian distance matrix for hierarchical sample grouping. Based on the most similar transcriptome profile determined by a single linkage method, a dendrogram and a heatmap were created, relating sample expression profiles of Desirée WT (D-WT) versus Desirée O6 (D-O6) and 01H15-WT (H-WT) versus 01H15 WT-O6 (H-O6) into colors ranging from red (identical profiles) to blue (the most different profiles). Genes implicated in terpenoid, and carotenoid, plant hormone, and starch pathways were identified using the two database annotations.

2.8 | qRT-PCR analysis

To perform qRT-PCR analysis, 2 μg of total RNA was treated with RQ1 DNase (Promega) and reverse transcribed using oligo dT primers. In the meantime, RT from 1 to 2 μg of total RNA was used to synthesize first-strand cDNAs using a GE Healthcare Life Sciences (Buckinghamshire, UK) first-strand cDNA synthesis kit and 18mer oligo dT primers. Primer Express software was used for primer design. Supplemental Table S2 lists the primers used for carotenoid and apocarotenoid analyses. A StepOne™ Thermal Cycler (Applied Biosystems, Foster City, California, USA) was used to conduct real-time PCR, and StepOne Software v2.0 (Applied Biosystems, Foster City, California, USA) was used for analysis. The protocol was as follows: 5 min of initial denaturation at 94°C; 30 cycles of denaturation for 20 seconds at 94°C, 20 seconds of annealing at 60°C, and 20 seconds of extension at 72°C; and 5 minutes of final extension at 72°C. StepOne Software v2.0 (Applied Biosystems) was used for analysis after assays were completed in a StepOne™ Thermal Cycler (Applied Biosystems). For expression analysis, two technical replicates and three biological replicates were carried out. Using the 2- $\Delta\Delta\text{Ct}$ approach, changes in gene expression were calculated by normalizing each gene to elongation factor 2 (first Δ), and then calculating each gene's expression by comparing it to the normalized expression (second Δ).

2.9 | Statistical analysis

Three biological replicates were used for apocarotenoid and carotenoid analyses. Volatile analyses and data are presented as mean \pm SD. The significance between the treatments was tested by one-way ANOVA and Dunnett's Multiple Comparison Test using the GraphPad Prism Version 5.00.

3 | RESULTS AND DISCUSSION

Recently, potato plants have been engineered to specifically produce in their tubers the compounds responsible for the color, flavor, and aroma of saffron, namely crocins, picrocrocin, and safranal. By combining three genes from *Crocus sativus*, *CsCCD2L* with *UGT74AD1*, and *UGT709G1*, all driven by the patatin promoter, The modified transgenic potato tubers exhibited an accumulation of crocins and picrocrocin of 360 $\mu\text{g/g}$ DW and 800 $\mu\text{g/g}$ DW, respectively.²³ Nonetheless, the concentrations of these metabolites were far from the 14 mg/g of crocins obtained in ripe transgenic tomatoes.²¹ Therefore, the main goal of this research was to further increase the amount of crocins using a new potato background. Contrary to the low levels of carotenoids in *S. tuberosum* Desirée dominated by violaxanthin and lutein, *S. tuberosum* Group Phureja 01H15 WT accumulates a high content of total carotenoid, ca. 80% of which is zeaxanthin.³³

3.1 | Carotenoid and apocarotenoid content in transgenic tubers

Previously, *S. tuberosum* cv Desirée was successfully engineered to accumulate crocins and other apocarotenoids found in saffron, such as picrocrocin and its degradation product safranal. Beside their roles in plant, these apocarotenoids have bioactive qualities with a variety of medicinal and pharmacological uses.²³ This transgenic line was generated

by expressing three genes of saffron: *CsCCD2L*, *UGT74AD1* and *UGT709G1*, under tuber-specific promoter. The same strategy used in *S. tuberosum* cv Desirée, was followed in this study using the background *S. tuberosum* Group Phureja 01H15WT (H-WT). Since *CsCCD2L* can hydrolyze zeaxanthin at 7,8:7',8' double bonds to form crocetin dialdehyde and two molecules of 4-hydroxy-2,6,6-trimethyl-1-cyclohexene-1-carboxaldehyde (HTCC), this background was chosen to increase the quantity of crocins in potato tubers. Six independent transgenic lines of *S. tuberosum* Group Phureja 01H15WT-O6 (H-O6) were generated (Figure 1), and the genomic DNA was checked for the presence of the *CsCCD2L* transgene cassettes by PCR. Two positive lines were selected for further analyses, named lines 01H15WT-O6-1 (H-O6-1) and 01H15WT-O6-2 (H-O6-2).

By using HPLC-APCI-HRMS, the transgenic tubers and their corresponding controls were examined for the presence of carotenoids. In WT tubers, antheraxanthin, zeaxanthin, violaxanthin, neoxanthin, phytoene and phytofluene were identified, being zeaxanthin the main carotenoid detected. No variations were observed in violaxanthin and neoxanthin in transgenic lines (Table 1). In contrast, a dramatic drop was observed in the concentration of antheraxanthin and zeaxanthin, which resulted in 6 and 30-fold lower contents in comparison to WT, respectively. On the other hand, the amount of phytoene and phytofluene increased by 9 and 15-fold, respectively, thus showing that the carotenoid pool used to produce crocetin, picrocrocetin, and crocins is somehow diminished by the presence of *CsCCD2L*, influencing the accumulation of carotenoids produced during the first stages of the metabolic pathway (Table 1).

Polar extracts from the two lines expressing the O6 construct were analyzed for de novo synthesis of the major saffron apocarotenoids. In this study, HPLC-DAD was used to identify and quantify the amounts of crocins using the method reported by Diretto et al.³⁴ All the typical apocarotenoids of saffron could be found in the two lines, albeit in varied concentrations when compared to the crocin profile of saffron. High amounts of crocins, were accumulated by all transgenic tuber potato lines such as crocin 1 [(crocetin-(β -D-glucosyl)-ester)], crocin 2 [(crocetin-(β -D-glucosyl)-(β -D-glucosyl)-ester], crocin 3 [(crocetin-(β -D-gentiobiosyl)-(β -D-glucosyl)-ester)], and with trans-crocetin 2 being the main type of crocins found in these tubers (Figure 2). Moreover, the amounts of picrocrocetin and its precursor HTCC in WT and transgenic tubers were examined. Of note, picrocrocetin and HTCC were found in the two lines but were not detected in the WT tuber (Figure 2).

By using GC-MS, safranal and other volatile apocarotenoid compounds were analyzed. Five distinct volatiles produced from carotenoids were found (Table 2). In particular, safranal, a novel metabolite for potato harboring the O6 construct identified in the two transgenic lines, was revealed to be the product of the 7,8:7',8' cleavage activity over



FIGURE 1 Potato group phureja 01H15 (H) and Desirée (D) wild type and transgenic line accumulating the characteristic apocarotenoids in saffron.

TABLE 1 Carotenoids identified and quantified in tubers of H-WT and H-O6 transgenic lines. Data are expressed as fold internal standard (IS). The statistical differences between the mean values of the transgenic lines in comparison to the control are shown by their *p*-value. *p*-values lower than 0.01 and 0.005 are flagged with (**) (***) respectively.

Carotenoid	H-WT AVG \pm SD	H-O6-1 AVG \pm SD	H-O6-2 AVG \pm SD
Neoxanthin	0.038 \pm 0.006	0.031 \pm 0.009	0.034 \pm 0.007
Violaxanthin	0.064 \pm 0.015	0.018 \pm 0.004**	0.023 \pm 0.009**
Antheraxanthin	0.394 \pm 0.035	0.062 \pm 0.017***	0.054 \pm 0.007***
Phytoene	0.044 \pm 0.006	0.431 \pm 0.068***	0.378 \pm 0.081***
Phytofluene	0.014 \pm 0.002	0.226 \pm 0.030***	0.247 \pm 0.046***
Zeaxanthin	2.900 \pm 0.520	0.188 \pm 0.034***	0.164 \pm 0.042***

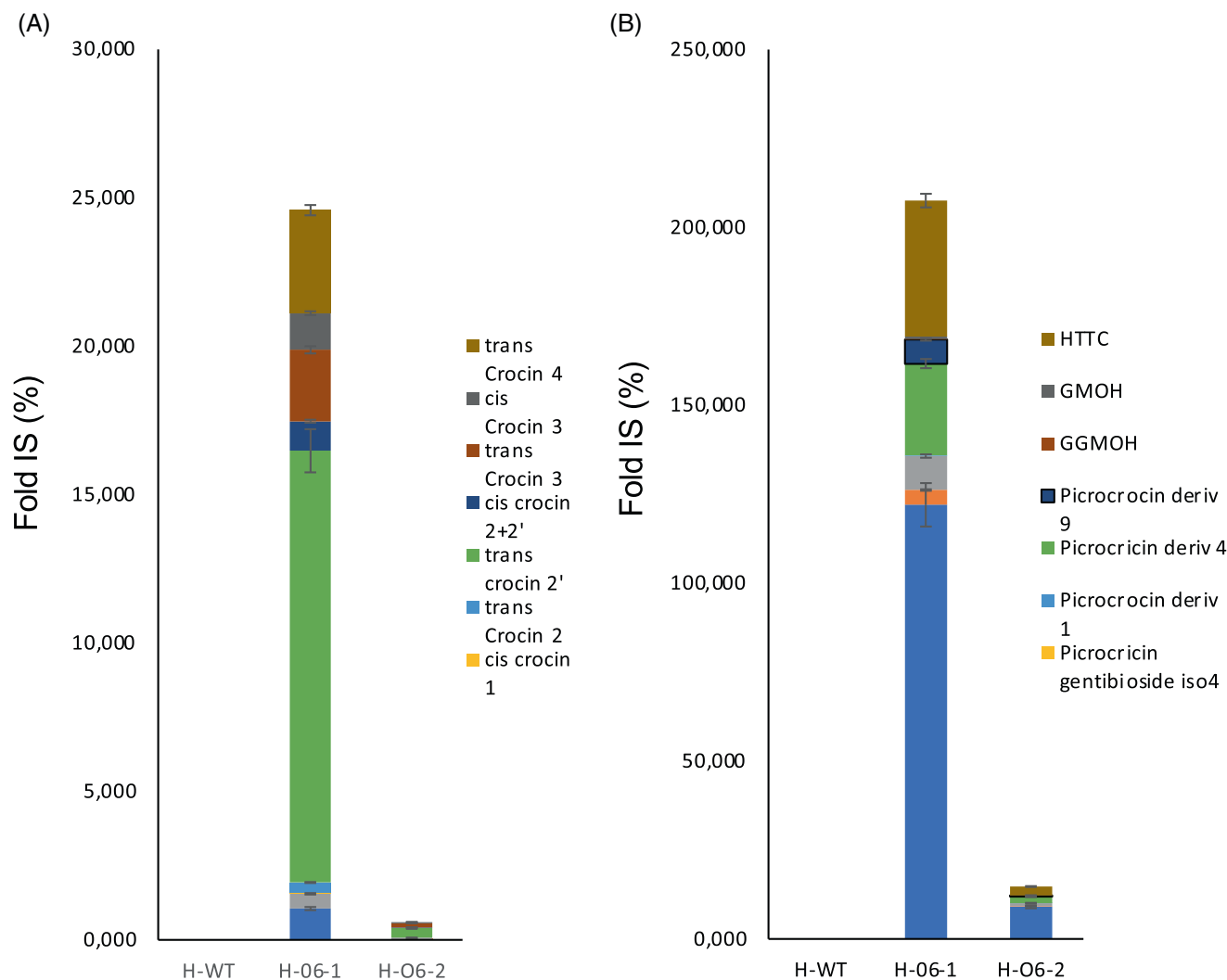


FIGURE 2 Metabolic engineering of saffron apocarotenoid in potato tuber. (A) Crocetin, crocins and picrocrocin contents in the WT and transgenic lines. (B) HTCC, and picrocrocin derivatives contents in the WT and transgenic lines. Data are averages \pm SD of three biological replicates and expressed as % of fold internal standard (IS) levels.

zeaxanthin. Other volatile apocarotenoids produced by the activities of CCD1 and CCD4, such as β -damascenone, geranylacetone and β -ionone, accumulate in the two transgenic lines at similar levels. Overall, the transgenic potato H-O6-1 accumulated a high content of these apocarotenoids, reaching 3.64 mg/g DW of crocins and 2.34 mg/g DW of picrocrocin.

The developed potato accumulated a high content of crocins and picrocrocin (3.64 mg/g DW, 2.34 mg/g DW, respectively) 10 and 3-fold up respectively in comparison to their levels in the Désirée background (0.360 mg/g DW and 0.800 mg/g DW) using the same construct. Up to now, the most efficient engineered system to produce crocins and picrocrocin has been described in the tomato fruit of stably transformed plants, where the levels of crocins attained up to 14.48 mg/g DW,²¹ succeeded by a transient tobacco system that employed CsCCD2L expression driven by a virus, allowing 8.24 ± 2.93 mg/g DW of picrocrocin and 2.18 ± 0.23 mg/g DW of crocins to accumulate.³⁵ In potato tubers Désirée, the major carotenoid types are violaxanthin and lutein while *S. tuberosum* Group Phureja 01H15 WT shows a high concentration of zeaxanthin, which would explain the increase in the accumulation of apocarotenoid metabolites in this genetic background when the same *CsCCD2L* and glycosyltransferases are used. This is the first time that engineered potatoes have been obtained accumulating exotic secondary metabolites in amounts of mg per g of dry weight. Previous attempts overexpressing different genes aiming to enhance the carotenoid content have only been able to accumulate amounts of 11–47 μ g/g DW.^{36,37}

TABLE 2 Volatiles emitted by tuber potatoes of 01H15WT and 01H15WT-O6 transgenic lines. Results are shown as the ratio of transgenic lines versus WT.

Compounds	H-O6-1	H-O6-2	H-WT
6-methyl-5-hepten-2-one	1.14 ± 0.24	1.13 ± 0.17	1.00 ± 0.22
Safranal*	1.67 ± 0.54	1.28 ± 0.49	NA
β-damascenone	0.95 ± 0.07	0.84 ± 0.18	1.00 ± 0.13
Geranylacetone	1.45 ± 0.40	1.47 ± 1.44	1.00 ± 0.40
β-ionone	1.29 ± 0.11	1.46 ± 0.44	1.00 ± 0.13

Note: Analysis was done on three plants per line. Three conclusions can be found in the standard error (SD). NA, not relevant.

*The ratio of transgenic lines to line H-O6-2, which had the lowest levels of this metabolite of all the lines examined, was determined since this molecule was undetectable (NA) in H-WT potatoes. No statistically significant differences were found in the comparison of WT versus transgenic lines.

The presence of CsCCD2L in transgenic tubers pointed out that this protein can divert the metabolic flux toward the production of these apocarotenoids, and a similar behavior was observed in engineered Money Maker and hp3/B^{sh} tomato and Desirée potato.^{21,23,24}

Although potato H-O6 can accumulate crocins, their profiles differ from those of saffron stigmas: whereas in the transgenic potato, the major crocins are trans-crocin 2, trans-crocin 4 and trans-crocin 3, saffron stigmas are distinguished by the presence, in decreasing order of accumulation, of trans-crocin 4, trans-crocin 3, and trans-crocin 2. A different pattern of crocins has also been observed in different systems.^{21–23,35}

3.2 | Analysis of ABA and α-tocopherol levels in tubers

The amounts of isoprenoid other than carotenoids can sometimes be affected by the overexpression of different carotenogenic genes in plant tissues.^{37,38} To test whether comparable effects might be seen in potato tubers, the levels of ABA and α-tocopherol were measured in developing tubers from the H-O6-1 and 2 lines and the H-WT control. In the tubers of the two transgenic lines, ABA levels were within the range of values found in tubers from the control line (Table 3), suggesting that carotenogenic overexpression genes did not significantly affect ABA levels in potato tubers. However, H-O6-2 transgenic line growing tubers had an approximately 4-fold rise in α-tocopherol levels while δ-tocopherol was decreased. In line H-O6-1 the levels of the different tocopherols were slightly increased (Table 3). These findings suggest that the overexpression of carotenogenic genes may have differential effects on the levels of non-carotenoid isoprenoids in potato tubers. Although ABA levels remained relatively unaffected, α-tocopherol levels showed a significant increase in one of the transgenic lines. Studies have demonstrated that transgenic potato lines with increased α-tocopherol show excellent antioxidant capabilities.^{39–41} Because these transgenic lines are efficient at scavenging singlet oxygen and other cellular free radicals, and they have shown an increased capacity to survive a variety of abiotic stresses. These lines have higher tocopherol contents, which is associated with an antioxidant defense mechanism that is essential for maintaining the integrity and functionality of cellular membranes, especially in stressful situations. α-tocopherol contribute to the general resilience of transgenic potato plants by strengthening the cellular antioxidant defense system, which helps the plants better handle environmental challenges. This highlights the complexity of metabolic pathways and the potential for gene manipulation to influence metabolite profiles in plant tissues.

3.3 | Expression of transgenes in Desirée and 01H15

To determine the expression of the transgenes in both backgrounds containing the O6 construct, qPCR analysis was carried out. The three transgenes were expressed in both lines, although the degree of CsCCD2L expression in D-O6 was approximately 15 times higher than that in H-O6. This behavior was also seen in the other two crocus genes introduced in potato under the control of the patatin promoter, namely CsUGT74AD1, and CsUGT709G1, showing that the selected promoter pPAT was much stronger in the Desirée background than in 01H15 (Figure 3). Sucrose has been reported as a potent stimulator of potato tuberization. As a result, it appears reasonable that sucrose would promote the accumulation

TABLE 3 ABA and α -tocopherol levels detected in H-WT and H-O6 transgenic lines. Results are shown as the ratio of transgenic lines versus WT. The statistical differences between the mean values of the transgenic lines in comparison to the control are shown by their *p*-value. *p*-values smaller than 0.01 and 0.005 are flagged with (**) (***) respectively.

Compounds	H-O6-1	H-O6-2	H-WT
Dihydrophaseic acid	1.11 \pm 0.07	1.41 \pm 0.05 ***	1.00 \pm 0.04
ABA	1.23 \pm 0.06**	1.32 \pm 0.08**	1.00 \pm 0.02
α -tocopherol	1.21 \pm 0.09	4.07 \pm 0.23***	1.00 \pm 0.07
δ -tocopherol	1.21 \pm 0.12	0.37 \pm 0.03***	1.00 \pm 0.10
α -tocotrienol	1.15 \pm 0.06	1.03 \pm 0.05	1.00 \pm 0.08

Note: For each line, three plants were examined. Standard error (SD) indicates three determinations.

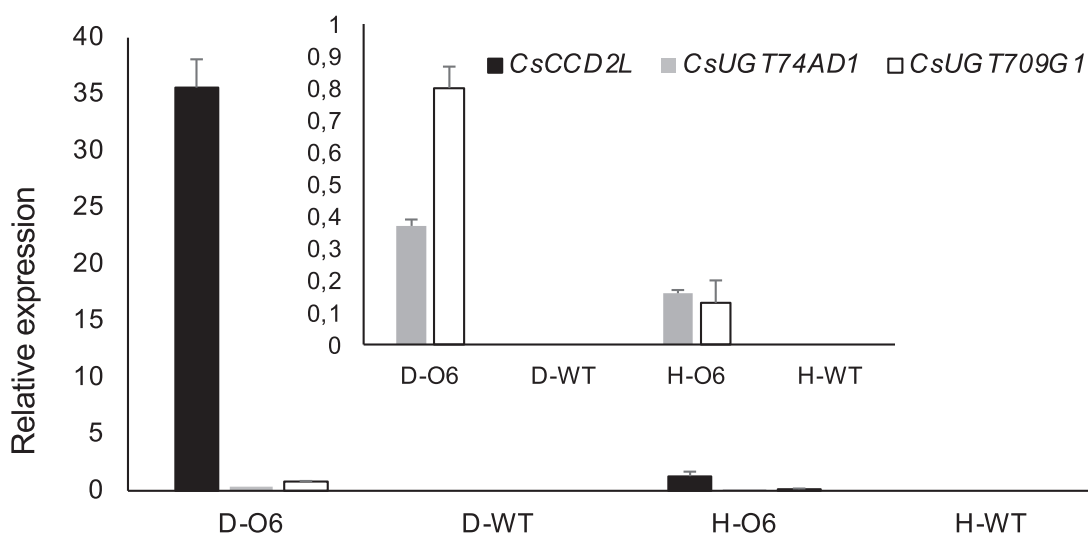


FIGURE 3 Relative expression of CsCCD2L, CsUGT2 and CsUGT709G1 genes in transgenic and wild type potato tubers from Desirée and 01H15WT. qRT-PCR was performed in triplicate with three biological repeats.

of the basic tuber protein patatin. However, light and phytohormones, in addition to sugar, influence tuber formation.⁴² Besides the high amount of crocins in H-O6, the low CCD expression driven by the pPAT promoter as compared to the Desirée background showed here suggests that there is room for further improvement in crocin /picrocrocins and safranal in the Phureja background. On the one hand, the expression of the *CsUGT* genes was too low in comparison to *CsCCD2L* expression and a more balanced expression of all the genes in the expression cassette (CCD and UGTs) would be desirable. The observed differences at the level of promoter performance in the two backgrounds suggested that the organ/tissue-specific promoters should be re-evaluated at the expression levels of each genetic background. Finally, it is possible that using the same promoter repeatedly to drive the three transgenes may be the cause of low transgene expression of the two UGT and the *CsCCD2L* genes. Thus, there is a need for alternative promoters with similar expression levels, and the transcriptome could be a valuable tool to search for these promoters.

Another alternative to improve further the accumulation of these metabolites, would be boosting the isopentenyl diphosphate (IPP) and dimethylallyl diphosphate (DMAPP) production flux in potato. Plants use two main metabolic processes to produce IPP and DMAPP, which are building blocks for the biosynthesis of terpenoids: the MEP pathway in plastids and the MVA pathway in the cytosol.⁴³ A viable method for increasing the synthesis of terpenoid chemicals downstream is plant modification through the introduction of exogenous MVA pathway genes. For instance, cytoplasmic IPP/DMAPP production is shown to rise when exogenous HMG-CoA reductase (HMGR) is added to the tobacco leaves' cytoplasm. The plant can then express exogenous genes involved in carotenoid biosynthesis, such as crtB, crtE, and crtI, to increase its accumulation of carotenoid pigments, using the excess IPP/DMAPP.⁴³ It would be advantageous to include HMGR in the O6 construct to further improve our platform. Pérez et al.⁴⁴ pointed out, altering the flow of the MEP plastid

pathway can have more potent, pleiotropic consequences. These effects are probably caused by hormones generated from plastid IPP/DMAPP by growing plants. Basallo et al. suggested that an orthogonal MVA pathway in plastids may be a more efficient technique to boost the production of IPP/DMAPP exclusively within chloroplasts while reducing any negative impacts on plant development.⁴⁵ This approach may provide a more focused and effective way to improve plant terpenoid production and consequently crocin accumulation.

3.4 | Transcriptome analysis

To obtain insights on the effect of construct O6 in potato tubers, four RNA samples were used for transcriptomic analyses, including Desirée WT (D-WT) and 01H15-WT (H-WT) as controls and the corresponding lines carrying the O6 construct (D-O6 and H-O6). RNA sequencing of the D-O6, D-WT, H-O6, and H-O6 lines yielded 116,729,882; 110,616,682; 104,743,074; and 110,009,782 raw pair-end reads, respectively, with a ratio of bases with quality score greater than or equal to 30 (Q30) greater than 95% in all cases. The Trimmomatic program was used to remove adapter sequences and bases with base quality lower than three from the ends and the sliding window method was used to trim bases of reads that do not qualify for window size 4, and mean quality 15.²⁹ Afterwards, reads with a length shorter than 36 bp were dropped to produce trimmed data. In D-WT and D-O6, 109,350,216 and 115,221,756 reads were finally produced, and total read bases were 15.5Gbp and 16.3Gbp, respectively. The GC content (%) was 51.49% and 52.44% and Q30 were 96.25% and 96.48%, respectively. However, in H-WT and H-O6 108,658,198 and 103,377,642 reads were obtained, and total read bases were found to be 15.4Gbp and 14.6Gbp, respectively. The GC content was very similar ranging from 50.73% and 52.17%. Q30 were 96% in both samples. Each sample's trimmed readings have been assembled into a single file to provide a unified reference. To perform de novo assembly, Trinity³¹ was employed with default settings, resulting in 146,004 transcript contigs. Subsequently, the longest contigs of the assembly were grouped into non-redundant transcripts (unigenes) using CD-HIT-EST.³⁰ Unigenes were further used for ORF prediction and annotation. The statistics of these assembled transcript contigs, such as the total number of genes and transcripts, GC content in percentage, and N50 value, are presented in Table 4.

3.5 | Functional annotation

In order to perform functional annotation, unigenes were searched against Kyoto Encyclopedia of Genes and Genomes (KEGG), NCBI Nucleotide (NT), Pfam, Gene ontology (GO), NCBI non-redundant Protein (NR), UniProt and EggNOG using BLASTN of NCBI BLAST and BLASTX of DIAMOND software with an E-value default cutoff of 1.0E-5. The results are listed in Table 5. Among a total of 129,503 unigenes retrieved, 119,187 genes were annotated, with NT obtaining the greatest percentage at 89.7% and UniProt obtaining the lowest at 21.5% (Table 5).

TABLE 4 Statistics after merged assembly from all four analyzed samples.

Assembly	Merge	
	ALL transcript contigs	Only longest isoform per "GENE"
Total trinity "genes"	146,004	146,004
Total trinity transcripts	217,765	146,004
Percent GC	38.67	38.13
N50	1115	873
Maximum contig length	18,669	18,669
Minimum contig length	201	201
Median contig length	447.0	384.0
Average contig length	734.88	628.85
Total assembled bases	160,031,007	91,814,827

TABLE 5 Annotation results of various databases.

Assembly	Merge
Total Unigene	129,503
GO	34,566 (26.69%)
UniProt	27,863 (21.52%)
NR	48,234 (37.25%)
Pfam	31,702 (24.48%)
EggNOG	48,930 (37.78%)
NT	116,261 (89.77%)
KO_EUK	46,473 (35.89%)
Overall	119,187 (92.03%)

Figure S1 displays the gene ontology annotation of the assembled unigenes from the newly developed tuber transcriptome. In all, 34,566 transcripts have been given at least one GO Slim term in the categories of biological process (3100), molecular function (3211), and cellular component (2913). The protein metabolism process (33.2%) was the most represented biological process term, followed by cellular process (14.4%), biological regulation (12.9%), response to stimulus (10.4%), localization (7.4%), developmental process (3.1%), cell organization and biogenesis process (2.5%), and multicellular organismal process (1.1%). (Figure S1a). The cellular component category is shown in Figure S1b, with the subcategories cell part (45.3%), organelle (22.8%), membrane part (8.5%), membranes (7.5%), protein-containing complex (5.9%), organelle part (3.7%), extracellular region (2.3%), and cell junction (1.3%) being the most prevalent subcategories. Catalytic activity (45.5%) and binding (33%), transport activity (4.9%), transcription regulator activity (3.6%), structural molecule activity (1.9%), and molecular function regulator (1%) were the terms with the highest frequency under molecular function (Figure S1c).

The EdgeR software was used to perform assessments of differential expression.³² Rather than providing individual quantifications, normalization was performed for the sample types to provide the correct differential expressions. Figure S2a displays the distribution of the normalized expression level. By considering the sequencing depths reflected by library sizes, the EdgeR software adjusted the analysis. To identify changes among samples, a multidimensional scaling (MDS) plot was created using differences between the samples from the transcriptome analysis (Figure S2b). This makes it possible to find proof of the spatial arrangement that demonstrates how similar or different the tuber samples are from one another. The plot shows that while 67.3% of the variations in gene expression were caused by the presence or absence of the construct O6 in the examined samples, 21.1% of the variances between samples were caused by the potato varieties.

DEGs were analyzed by comparing the WT and transgenic tubers for each background. After data preprocessing and low-quality transcript filtering, 31,262 contigs were used for TMM Normalization. Significant DEGs were identified based on the statistical significance ($p \leq 0.05$) and $\geq 2 \log_2$ fold change (FC) for up-regulated, and $\leq -2 \log_2$ FC values for down-regulated genes. 1405 (up-regulated) and 1252 (down-regulated) of the 2657 genes with differential expression in Desirée were significant DEGs. On the other hand, out of the 5107 genes that were differently expressed in the 01H15 background, 2586 were up-regulated and 2521 were down-regulated significant DEGs.

3.6 | Analysis of gene expression participating in terpenoid and carotenoid biosynthesis

Based on transcriptome analysis, variety accounted for 21.1% of sample variances, while the presence or absence of construct O6 in the studied samples accounted for 67.3% of gene expression differences. In addition, this result indicated that the expression of genes in construct O6 and/or the accumulation of crocins are factors affecting not only the biosynthesis of carotenoids but probably other pathways. Our first focus was on the analysis of the terpenoid pathway. Monoterpene and diterpene precursors originate in plastids via the MEP pathway, whereas sesquiterpene and triterpene precursors originate in the cytoplasm via the MVA pathway.

All the genes involved in the upstream of the pathway were upregulated in H-O6, except the hydroxymethylglutaryl-CoA reductase *HMGCR* (c103119_g1_i1), which was downregulated. Contrarily, in Desirée D-O6, hydroxymethylglutaryl-CoA reductase *HMGCR* (c95949_g2_i2), phosphomevalonate kinase *mvaK2* (c84034_g1_i2) and Mevalonate Diphosphate Decarboxylase *MVD* (c87616_g1_i3) were downregulated while the remain genes were upregulated. The expression of Farnesyl Diphosphate Synthase *FDPS* (c73495_g1_i3) in both background remained invariable (Figure 4).

At the level of the specific carotenoid pathway, both background showed the same pattern except for carotene hydroxylase *CHY2* (c67024_g1_i1) and 9-cis-epoxycarotenoid dioxygenase *NCED* (c70455_g1_i1), where the transcript were upregulated in H-O6 and downregulated in D-O6, 9-cis-epoxycarotenoid dioxygenase *NCED* (c89174_g1_i1) and Aldehyde oxidase 3 *AAO3* (c57491_g1_i2) remain unchanged (Figure 4). When the two rate-limiting enzymes, *HMGCR* and *DXS* were considered, they each played substantial roles in the overall control of the MVA and MEP pathways. *HMGCR* was found to be less abundant in D-O6 and H-O6. IPTS enzymes are the main enzymes that connect the downstream isoprenoid biosynthesis branch points of diverse structures to the upstream MVA and MEP pathways. In higher plants, the key enzymes *GPPS*, *GGPPS*, *FPPS*, and *CPPS* involved in the production of isoprenoid metabolites have recently been identified. These genes were upregulated in D-O6 but downregulated in H-O6, indicating different responses of the two backgrounds to the presence of the O6 construct. Nevertheless, we should also consider the differences at the metabolite level. Most of the research revealed a strong correlation between the levels of these gene transcripts and the presence of their respective terpenoids.⁴⁶

The genes involved in ABA signal transduction showed a similar behavior in both backgrounds except for the plant hormone receptor *PYL* (c84221_g1_i1) and abscisic acid-responsive transcription factor *ABF* (c79438_g1_i1) genes, which were increased in D-O6 and H-O6, and decreased in D-O6 and H-O6, respectively. The remaining genes (Figure 4) either exhibited high expression or remained stable. ABA levels were lower in D-O6 than in H-O6.²³ Nevertheless, these data should not be taken isolated and consider as well the absolute expression levels of the other *NCED* genes, in addition to other enzymes involved in ABA metabolism. ABA biosynthesis starts with isoprenoids from the plastidic methyl-D-erythritol-4-phosphate (MEP) pathway.⁴⁷ Zeaxanthin is the particular carotenoid that promotes ABA production. Indeed, 9'-cis-neoxanthin and 9'-cis-violaxanthin, the universal ABA precursors, may be formed from neoxanthin and violaxanthin, respectively. The conversion of 9'-cis-neoxanthin and 9'-cis-violaxanthin into xanthoxin by the 9-cis-epoxycarotenoid dioxygenase (*NCED*) family of enzymes is considered the first committed step in ABA biosynthesis and is rate limiting.⁴⁸

3.7 | Analysis of genes participating in plant hormone biosynthesis

Numerous physiological alterations occur when potato tubers emerge from dormancy. The change in metabolic balance toward catabolism, which indicates the start of growth and development, is one important feature. An increase in DNA and RNA production frequently coincides with this metabolic change, indicating increased cellular activity as the tuber gets ready to sprout and expand. Furthermore, the ratios of important phytohormones, specifically gibberellins (*GA*) and abscisic acid (*ABA*), as well as *ABA* and cytokinins (*CK*), are dynamically altered. These variations in hormone ratios are important regulators of many aspects of development and dormancy, coordinating intricate signaling pathways that control physiological functions inside the tuber.⁴⁹ In order to cause bud rupture and start the sprouting process in tubers, *CKs* are essential. Endogenous zeatin is a naturally occurring cytokinin, and its content rises noticeably during the shift from dormancy to active growth. The sudden elevation of zeatin levels in the bud tissues is a critical signal for inducing cell division and growth activities. Simultaneously, abscisic acid (*ABA*), another important phytohormone involved in maintaining dormancy, is frequently seen to be at lower levels. The shift from dormancy to active development is further reinforced by the reduction in *ABA*, which also creates a hormonal milieu that facilitates bud rupture and the start of sprouting.^{50,51} Therefore, the analyses of transcripts involved in *CKs* biosynthesis were performed. More in detail, the cytokinin trans-hydroxylase *CYP735A* (c91406_g2_i3) and isopentenyl transferase (*IPT*) (c95266_g1_i1) were found to be upregulated in both backgrounds carrying O6 (Figure 5). The cis-zeatin O-glucosyltransferase (*cisZOG*) genes, which belong to the O subfamily encoding a stereo-specific O-glucosylation of cis-zeatin-type cytokinins, did not show a clear pattern and some members were upregulated in H-O6 and downregulated in D-O6 (c64812_g1_i1), as depicted in Figure 5. Although the *IPT* primarily utilizes dimethylallyl diphosphate (*DMAPP*), ATP, or ADP, the principal starting product in

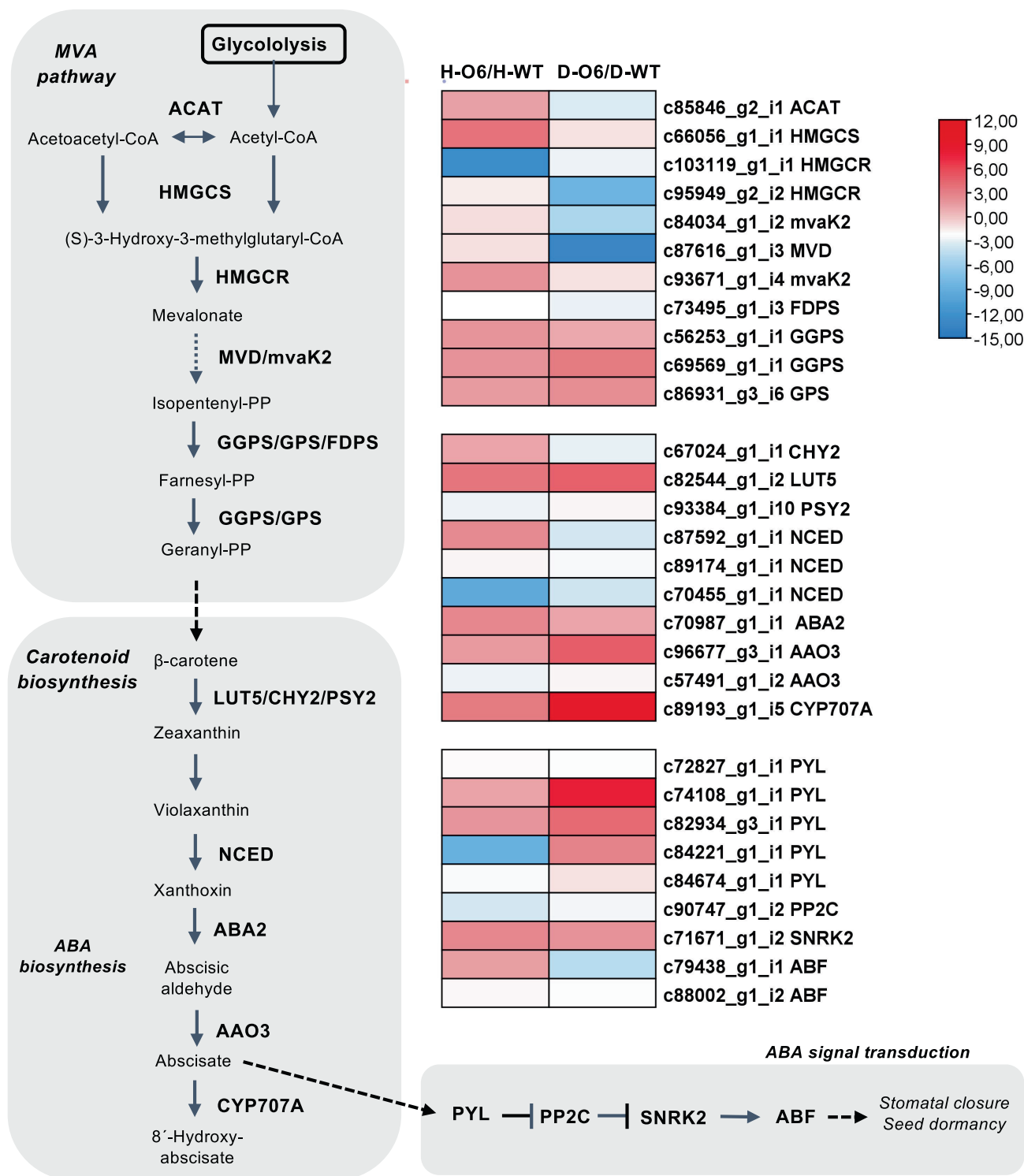


FIGURE 4 Terpenoid pathway and heatmap differentially expressed genes involved in terpenoid pathway. In the heat maps, each horizontal line refers to a gene. Relatively up-regulated genes are shown in red, whereas down-regulated genes are shown in blue.

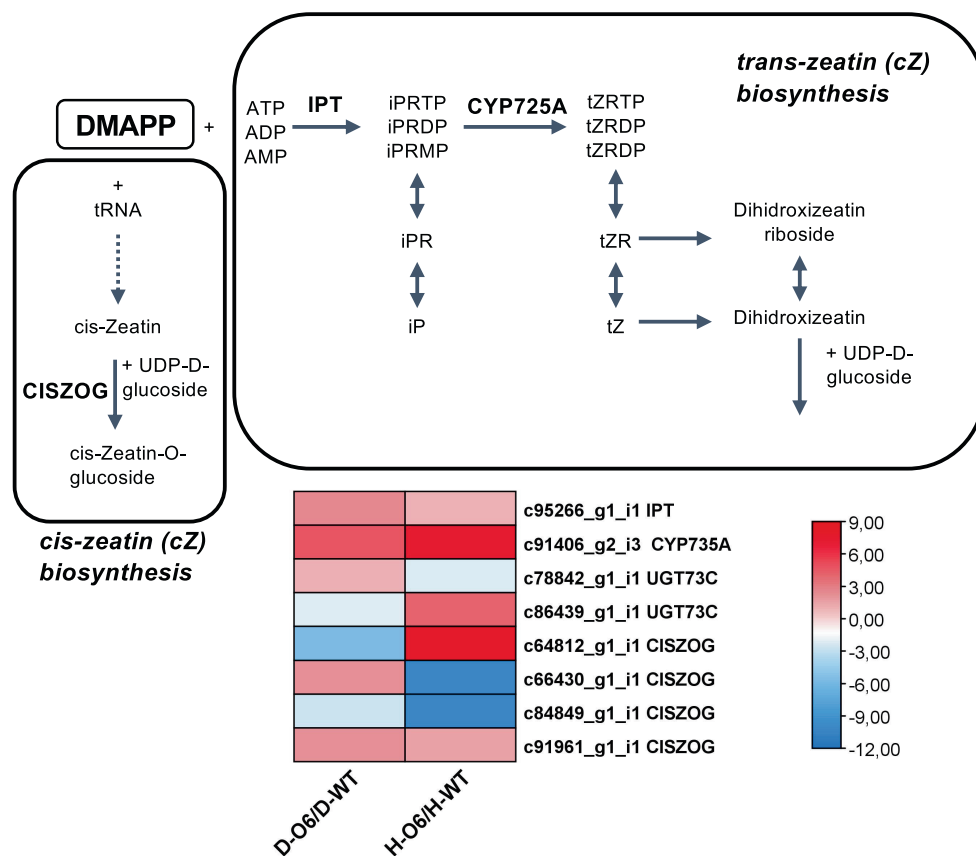


FIGURE 5 Plant hormone pathways and heatmap of differentially expressed genes. In the heat maps, each horizontal line refers to a gene. Relatively up-regulated genes are shown in red, whereas down-regulated genes are shown in blue.

higher plants is an iP nucleotide, such as iP riboside 5'-triphosphate (iPRTP) or iP riboside 5'-diphosphate (iPRDP).⁵² It is widely recognized that both biotic and abiotic stressors exert significant effects on IPT expression.⁵³ However, the response differs between biotic and abiotic stress conditions. Under biotic stress, endogenous levels of cytokinins tend to increase due to enhanced IPT expression. Conversely, exposure to abiotic stress typically leads to a reduction in endogenous CK levels, associated with decreased IPT expression. The magnitude and duration of the stress play crucial roles in determining the extent of this response.⁵⁴ The upregulation of cytokinin trans-hydroxylase and cytokinin synthase in D-O6 and H-O6 may have potential implications for enhancing plant resilience to environmental stressors and optimizing growth and development processes. Further research is warranted to elucidate the underlying mechanisms and potential implications of these findings.

3.8 | Expression analyses of genes participating in starch and sucrose metabolism

Unigenes involved in the biosynthesis and degradation of starch have been detected through coordinated enzymes in various pathways, starch and sucrose can be reversibly metabolized.⁵⁵ These enzymes include alpha-amylase (AMY), beta-amylase (BAM), starch phosphorylase (SP), ADP-glucose pyrophosphorylase (AGPase), starch synthases/granule-bound starch synthases (SS/GBSS), starch-branching enzyme (SBE or GBE) and starch debranching enzyme (DBE) for starch degradation and synthesis and sucrose-phosphate synthase (SPS), UDP-glucose pyrophosphorylase (UGPase), sucrose synthase (SuS), invertase (INV) and fructokinase (Frk) for sucrose synthesis and hydrolysis.

The potato varieties Désirée and Phureja differ in their starch content, which is responsible for the type and quality of starch produced in tubers. The amylose content affects its gelatinization and texture. The size of starch

granules affects the texture of cooked potatoes. Different gelatinization temperatures are exhibited between the two varieties, a chemical process in which starch absorbs water and swells when heated, resulting in the thickening or gelling of foods. Désirée potatoes have a higher gelatinization temperature, requiring more heat for the starch to fully gelatinize.

Different sets of genes involved in starch and sucrose metabolism appear to be more active in H-O6/H-WT than in D-O6/D-WT. Hexokinase (HK) (c70074_g1_i1 and c82627_g1_i3) and phosphoglucomutase (pgm) (c94954_g1_i2 and c90704_g5_i2), sucrose synthase (SUS) (c95044_g5_i1) starch-branching enzyme (c94540_g1_i2) and the granule-bound starch synthase I (GBSSI or waxy) (c91056_g1_i3) (Figure 6). These enzymes are involved in the earlier steps of glucose metabolism and play crucial roles in carbohydrate metabolism and energy production. They help regulate the flow of glucose and control its utilization within the potato cells. The upregulation of these genes in H-O6 is pointing out to an increase in the content of amylose in H-O6. On the other hand, the alpha-amylase (AMY) (c92039_g1_i1 and c94829_g1_i2) enzymes, which catalyze the hydrolysis of starch, seem to be upregulated in D-O6, suggesting the breakdown of starch in this variety.

A source of carbohydrates is necessary for carotenoid production in order to assemble the carotenoid molecular backbone. Plastids are the locations of carbohydrate metabolism, which is thought to be connected to the accumulation of carotenoid pigments. The up-regulation of SUS and INV is believed to improve the metabolic flow from the glycolytic pathway to the MEP pathway.⁵⁶ SUS and INV are the key enzymes that catalyze the conversion of sucrose to glucose and fructose in the glycolytic pathway.⁵⁷ These enzymes were up-regulated in the H-O6 background, which might enhance the metabolic flux from the glycolytic pathway into the MEP pathway.

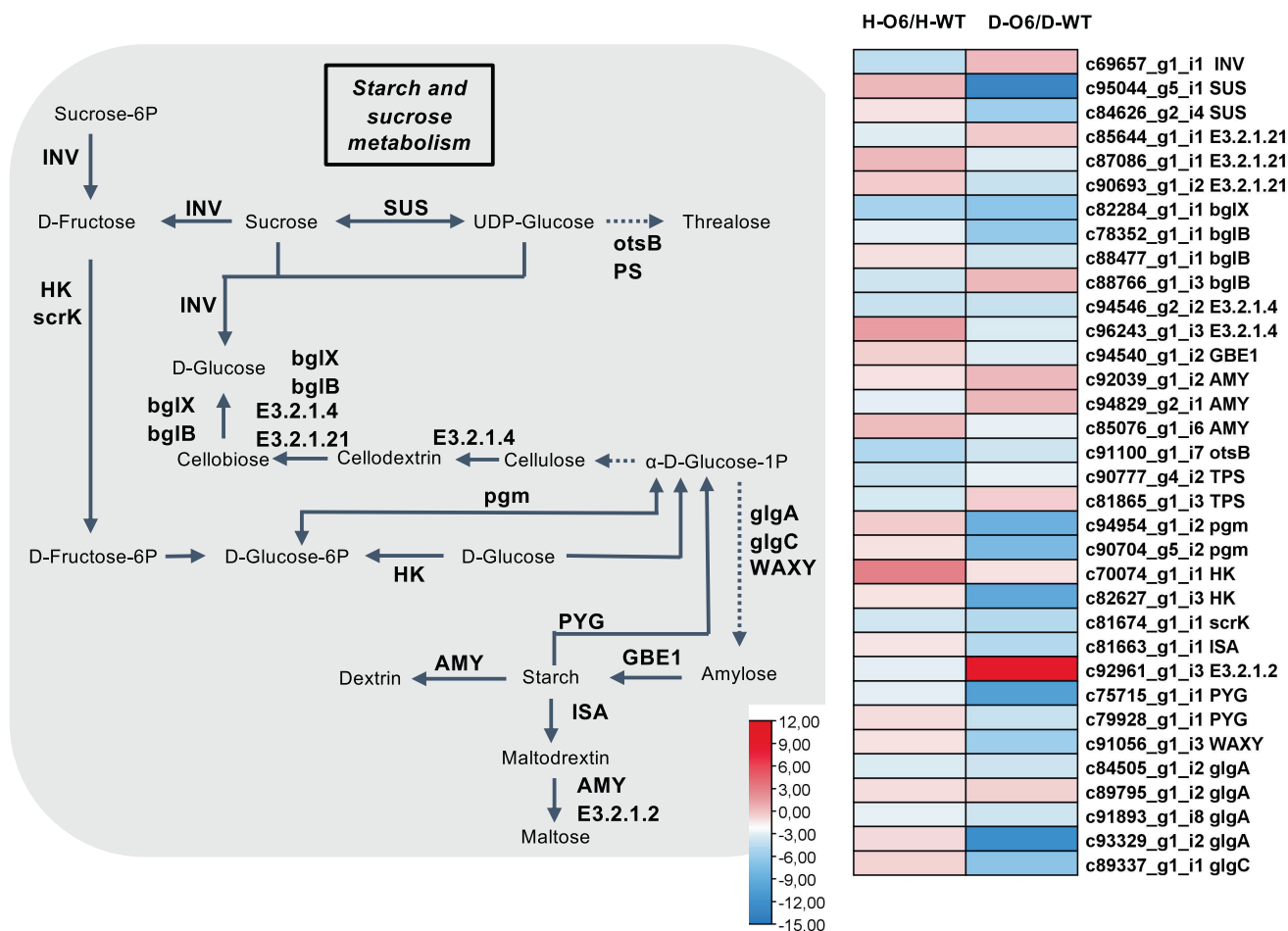


FIGURE 6 Starch and sucrose pathways and heatmap differentially expressed genes. In the heat maps, each horizontal line refers to a gene. Relatively up-regulated genes are shown in red, whereas down-regulated genes are shown in blue.

Desirée potatoes are known to have higher GBSS expression, resulting in a higher amylose content compared to Phureja potatoes, which typically have lower GBSS expression.⁵⁸ The presence of the construct O6 in H-O6 led to an increased expression of GBSS in this background. Probably H-O6 potatoes would have a firmer and less sticky texture when cooked in comparison to H-WT potatoes, which would contain a lower amylose content, leading to a softer and stickier texture. In contrast, Desirée potatoes typically have larger starch granules, resulting in a drier and more mealy texture, while Phureja potatoes have smaller starch granules, leading to a smoother and creamier texture.⁵⁹ The starch branching enzyme (SBE) genes are involved in the formation of amylopectin, the branched component of starch. Different SBE genes expression patterns can influence on the structure and properties of amylopectin. GBE1 gene was upregulated in H-O6 and downregulated in D-O6, indicating the formation of longer and more complex branching patterns within amylopectin in H-O6. Furthermore, D-O6 showed high levels of alpha-amylase activity, which can lead to undesirable effects. For example, during storage, excessive alpha-amylase activity can cause the breakdown of starch into sugars, resulting in a sweet taste and darkening of the potato flesh when cooked.

4 | CONCLUSION

Overall, we have shown that the concentration of crocins in engineered potatoes can be increased even further by using *S. tuberosum* Group Phureja with higher concentrations of the proper carotenoid precursors for crocin biosynthesis. The complexity of gene expression in Desirée and 01H15 carrying the O6 construct, as well as the connections among different pathways, were highlighted by the transcriptome sequence data, stressing the importance of considering different genetic backgrounds when carrying out metabolic engineering for the production of secondary metabolites. The introduction of the saffron mini-pathway into the Phureja potato variety affects several pathways; however, the plant's survival and phenotype remain unaffected. This heterologous system therefore emerges as a reliable and effective platform for the biosynthesis of these highly sought-after metabolites.

AUTHOR CONTRIBUTIONS

Lourdes Gómez-Gómez, Antonio Granell, and Oussama Ahrazem conceived and designed the research. Alberto José López-Jimenez, Lucía Morote, Enrique Niza, Ángela Rubio-Moraga, José Luis Rambla, Gianfranco Diretto, Sarah Frusciante, Javier Argandoña, Antonio Granell, Silvia Presa, Cristian Martínez Fajardo, Lourdes Gómez-Gómez, and Oussama Ahrazem conducted the experiments. Lourdes Gómez-Gómez, Antonio Granell, Gianfranco Diretto, and Oussama Ahrazem analyzed the data. Lourdes Gómez-Gómez, Antonio Granell, and Oussama Ahrazem drafted the manuscript. All authors reviewed and contributed to the final manuscript which was approved by all.

ACKNOWLEDGMENTS

We thank to Kathy Walsh for proofreading the article. Gianfranco Diretto and Lourdes Gómez-Gómez are participants of the European COST action CA15136 (EUROCAROTEN). Lourdes Gómez-Gómez is a participant of the CARNET network (BIO2015-71703-REDT and BIO2017-90877-RED). José Luis Rambla was supported by the Spanish Ministry of Science and Innovation through a “Juan de la Cierva-Incorporación” grant (IJC2020-045612-I). The UCLM and IBMCP groups constitute the Associated Unit CAROTENOID BIOTECHNOLOGY and TOMAFRAN.

CONFLICT OF INTEREST STATEMENT

The authors declare that they have no known competing financial interests or personal relationships that could have appeared to influence the work reported in this article.

PEER REVIEW

The peer review history for this article is available at <https://www.webofscience.com/api/gateway/wos/peer-review/10.1002/eng2.12997>.

DATA AVAILABILITY STATEMENT

Data will be made available on request.

ORCID

Oussama Ahrazem  <https://orcid.org/0000-0001-9183-9319>

REFERENCES

- Rodriguez-Concepcion M, Avalos J, Bonet ML, et al. A global perspective on carotenoids: metabolism, biotechnology, and benefits for nutrition and health. *Prog Lipid Res.* 2018;70:62-93. doi:10.1016/j.plipres.2018.04.004
- Ahrazem O, Gomez-Gomez L, Rodrigo MJ, Avalos J, Limon MC. Carotenoid cleavage oxygenases from microbes and photosynthetic organisms: features and functions. *Int J Mol Sci.* 2016;17(11):1781. doi:10.3390/ijms17111781
- Havaux M. Carotenoid oxidation products as stress signals in plants. *Plant J.* 2014;79(4):597-606.
- Sui X, Kiser PD, von Lintig J, Palczewski K. Structural basis of carotenoid cleavage: from bacteria to mammals. *Arch Biochem Biophys.* 2013;539(2):203-213.
- White MD, Flashman E. Catalytic strategies of the non-heme iron dependent oxygenases and their roles in plant biology. *Curr Opin Chem Biol.* 2016;31:126-135.
- Moreno JC, Al-Babili S. Are carotenoids the true colors of crop improvement? *New Phytol.* 2023;237(6):1946-1950.
- Liang M-H, He Y-J, Liu D-M, Jiang J-G. Regulation of carotenoid degradation and production of apocarotenoids in natural and engineered organisms. *Crit Rev Biotechnol.* 2021;41(4):513-534.
- Cataldo VF, López J, Cárcamo M, Agosin E. Chemical vs. biotechnological synthesis of C 13-apocarotenoids: current methods, applications and perspectives. *Appl Microbiol Biotechnol.* 2016;100:5703-5718.
- Li H-H, Hao R-L, Wu S-S, et al. Occurrence, function and potential medicinal applications of the phytohormone abscisic acid in animals and humans. *Biochem Pharmacol.* 2011;82(7):701-712.
- Fridlender M, Kapulnik Y, Koltai H. Plant derived substances with anti-cancer activity: from folklore to practice. *Front Plant Sci.* 2015;6:799.
- Ansari M, Emami S. β -Ionone and its analogs as promising anticancer agents. *Eur J Med Chem.* 2016;123:141-154.
- Rodriguez-Amaya DB. Carotenes and xanthophylls as antioxidants. *Handbook of Antioxidants for Food Preservation.* Elsevier; 2015: 17-50.
- Kloer D, Schulz G. Structural and biological aspects of carotenoid cleavage. *Cell Mol Life Sci.* 2006;63:2291-2303.
- dela Sena C, Riedl KM, Narayanasamy S, Curley RW, Schwartz SJ, Harrison EH. The human enzyme that converts dietary provitamin a carotenoids to vitamin a is a dioxygenase. *J Biol Chem.* 2014;289(19):13661-13666.
- Oberhauser V, Woolstra O, Bangert A, von Lintig J, Vogt K. NinaB combines carotenoid oxygenase and retinoid isomerase activity in a single polypeptide. *Proc Natl Acad Sci.* 2008;105(48):19000-19005.
- Alder A, Jamil M, Marzorati M, et al. The path from β -carotene to carlactone, a strigolactone-like plant hormone. *Science.* 2012;335(6074):1348-1351.
- Moiseyev G, Chen Y, Takahashi Y, Wu BX, Ma J-x. RPE65 is the isomerohydrolase in the retinoid visual cycle. *Proc Natl Acad Sci.* 2005;102(35):12413-12418.
- Ahrazem O, Rubio-Moraga A, Nebauer SG, Molina RV, Gomez-Gomez L. Saffron: its phytochemistry, developmental processes, and biotechnological prospects. *J Agric Food Chem.* 2015;63(40):8751-8764.
- Christodoulou E, Kadoglou NP, Kostomitsopoulos N, Valsami G. Saffron: a natural product with potential pharmaceutical applications. *J Pharm Pharmacol.* 2015;67(12):1634-1649.
- Gómez-Gómez L, Morote L, Fajardo CM, et al. Engineering the production of crocins and picrocrocin in heterologous plant systems. *Ind Crop Prod.* 2023;194:116283.
- Ahrazem O, Diretto G, Rambla JL, et al. Engineering high levels of saffron apocarotenoids in tomato. *Hortic Res.* 2022;9:uhac074. doi:10.1093/hr/uhac074
- Ahrazem O, Zhu C, Huang X, et al. Metabolic engineering of crocin biosynthesis in *Nicotiana* species. *Front Plant Sci.* 2022;13:861140. doi:10.3389/fpls.2022.861140
- Gomez Gomez L, Morote L, Frusciant S, et al. Fortification and bioaccessibility of saffron apocarotenoids in potato tubers. *Front Nutr.* 2022;9:1045979. doi:10.3389/fnut.2022.1045979
- Morote L, Lobato-Gómez M, Ahrazem O, et al. Crocins-rich tomato extracts showed enhanced protective effects in vitro. *J Funct Foods.* 2023;101:105432.
- Morris W, Ducreux L, Griffiths D, Stewart D, Davies H, Taylor M. Carotenogenesis during tuber development and storage in potato. *J Exp Bot.* 2004;55(399):975-982.
- Ahrazem O, Rubio-Moraga A, Berman J, et al. The carotenoid cleavage dioxygenase CCD2 catalysing the synthesis of crocetin in spring crocuses and saffron is a plastidial enzyme. *New Phytol.* 2016;209(2):650-663. doi:10.1111/nph.13609
- López AJ, Frusciant S, Niza E, et al. A new glycosyltransferase enzyme from family 91, UGT91P3, is responsible for the final Glucosylation step of Crocins in saffron (*Crocus sativus* L.). *Int J Mol Sci.* 2021;22(16):8815.
- Andrews S. FastQC: a quality control tool for high throughput sequence data. Babraham Bioinformatics, Babraham Institute, Cambridge, United Kingdom. 2010.
- Bolger AM, Lohse M, Usadel B. Trimmomatic: a flexible trimmer for Illumina sequence data. *Bioinformatics.* 2014;30(15): 2114-2120.

30. Grabherr MG, Haas BJ, Yassour M, et al. Full-length transcriptome assembly from RNA-Seq data without a reference genome. *Nat Biotechnol*. 2011;29(7):644-652.
31. Fu L, Niu B, Zhu Z, Wu S, Li W. CD-HIT: accelerated for clustering the next-generation sequencing data. *Bioinformatics*. 2012;28(23):3150-3152.
32. Robinson MD, McCarthy DJ, Smyth GK. edgeR: a Bioconductor package for differential expression analysis of digital gene expression data. *Bioinformatics*. 2010;26(1):139-140.
33. Campbell R, Morris WL, Mortimer CL, et al. Optimising ketocarotenoid production in potato tubers: effect of genetic background, transgene combinations and environment. *Plant Sci*. 2015;234:27-37. doi:10.1016/j.plantsci.2015.01.014
34. Diretto G, Ahrazem O, Rubio-Moraga A, et al. UGT709G1: a novel uridine diphosphate glycosyltransferase involved in the biosynthesis of picrocrocin, the precursor of saffranal in saffron (*Crocus sativus*). *New Phytol*. 2019;224:725-740. doi:10.1111/nph.16079
35. Martí M, Diretto G, Aragonés V, et al. Efficient production of saffron crocins and picrocrocin in *Nicotiana benthamiana* using a virus-driven system. *Metab Eng*. 2020;61:238-250. doi:10.1016/j.ymben.2020.06.009
36. Morris WL, Ducreux LJ, Fraser PD, Millam S, Taylor MA. Engineering ketocarotenoid biosynthesis in potato tubers. *Metab Eng*. 2006;8(3):253-263.
37. Ducreux LJ, Morris WL, Hedley PE, et al. Metabolic engineering of high carotenoid potato tubers containing enhanced levels of β -carotene and lutein. *J Exp Bot*. 2005;56(409):81-89.
38. Lindgren LO, Ståhlberg KG, Høglund A-S. Seed-specific overexpression of an endogenous Arabidopsis phytoene synthase gene results in delayed germination and increased levels of carotenoids, chlorophyll, and abscisic acid. *Plant Physiol*. 2003;132(2):779-785.
39. Gossett DR, Millhollon EP, Lucas MC. Antioxidant response to NaCl stress in salt-tolerant and salt-sensitive cultivars of cotton. *Crop Sci*. 1994;34(3):706-714.
40. Kumar D, Yusuf MA, Singh P, Sardar M, Sarin NB. Modulation of antioxidant machinery in α -tocopherol-enriched transgenic Brassica juncea plants tolerant to abiotic stress conditions. *Protoplasma*. 2013;250:1079-1089.
41. Upadhyaya DC, Bagri DS, Upadhyaya CP, Kumar A, Thiruvengadam M, Jain SK. Genetic engineering of potato (*Solanum tuberosum* L.) for enhanced α -tocopherols and abiotic stress tolerance. *Physiol Plant*. 2021;173(1):116-128.
42. Naumkina E, Bolyakina YP, Romanov G. Organ-specificity and inducibility of patatin class I promoter from potato in transgenic arabidopsis plants. *Russ J Plant Physiol*. 2007;54:350-359.
43. Andersen TB, Llorente B, Morelli L, et al. An engineered extraplastidial pathway for carotenoid biofortification of leaves. *Plant Biotechnol J*. 2021;19(5):1008-1021.
44. Pérez L, Alves R, Perez-Fons L, et al. Multilevel interactions between native and ectopic isoprenoid pathways affect global metabolism in rice. *Transgenic Res*. 2022;31(2):249-268.
45. Basallo O, Perez L, Lucido A, et al. Changing biosynthesis of terpenoid precursors in rice through synthetic biology. *Front Plant Sci*. 2023;14:1133299.
46. Srivastava Y, Tripathi S, Mishra B, Sangwan NS. Cloning and homologous characterization of geranylgeranyl pyrophosphate synthase (GGPPS) from *Withania somnifera* revealed alterations in metabolic flux towards gibberellic acid biosynthesis. *Planta*. 2022;256(1):4.
47. Finkelstein R. *Abscisic acid Synthesis and Response*. Vol 11. The Arabidopsis Book/American Society of Plant Biologists; 2013:11.
48. Emenecker RJ, Strader LC. Auxin-abscisic acid interactions in plant growth and development. *Biomolecules*. 2020;10(2):281.
49. Saidi A, Hajjibarat Z. Phytohormones: plant switchers in developmental and growth stages in potato. *J Genet Eng Biotechnol*. 2021;19(1):1-17.
50. Zhang X, Fujino K, Shimura H. Transcriptomic analyses reveal the role of Cytokinin and the nodal stem in microtuber sprouting in potato (*Solanum tuberosum* L.). *Int J Mol Sci*. 2023;24(24):17534.
51. Lomin SN, Myakushina YA, Kolachevskaya OO, et al. Global view on the cytokinin regulatory system in potato. *Front Plant Sci*. 2020;11:613624.
52. Hirose N, Takei K, Kuroha T, Kamada-Nobusada T, Hayashi H, Sakakibara H. Regulation of cytokinin biosynthesis, compartmentalization and translocation. *J Exp Bot*. 2008;59(1):75-83.
53. Ghosh A, Shah MNA, Jui ZS, Saha S, Fariha KA, Islam T. Evolutionary variation and expression profiling of isopentenyl transferase gene family in *Arabidopsis thaliana* L. and *Oryza sativa* L. *Plant Gene*. 2018;15:15-27.
54. Argueso CT, Ferreira FJ, Kieber JJ. Environmental perception avenues: the interaction of cytokinin and environmental response pathways. *Plant Cell Environ*. 2009;32(9):1147-1160.
55. Stein O, Granot D. An overview of sucrose synthases in plants. *Front Plant Sci*. 2019;10:95.
56. Li R-j, Hong Z, He S-z, Zhang H, Ning Z, Liu Q-c. A geranylgeranyl pyrophosphate synthase gene, IbGGPS, increases carotenoid contents in transgenic sweetpotato. *J Integr Agric*. 2022;21(9):2538-2546.
57. Ren Z, He S, Zhao N, Zhai H, Liu Q. A sucrose non-fermenting-1-related protein kinase-1 gene, IbSnRK1, improves starch content, composition, granule size, degree of crystallinity and gelatinization in transgenic sweet potato. *Plant Biotechnol J*. 2019;17(1):21-32.
58. Tuncel A, Corbin KR, Ahn-Jarvis J, et al. Cas9-mediated mutagenesis of potato starch-branching enzymes generates a range of tuber starch phenotypes. *Plant Biotechnol J*. 2019;17(12):2259-2271.

59. Ross HA, Wright KM, McDougall GJ, et al. Potato tuber pectin structure is influenced by pectin methyl esterase activity and impacts on cooked potato texture. *J Exp Bot.* 2011;62(1):371-381.

SUPPORTING INFORMATION

Additional supporting information can be found online in the Supporting Information section at the end of this article.

How to cite this article: Gómez-Gómez L, López-Jimenez AJ, Martínez Fajardo C, et al. Metabolic engineering of crocins and picrocrocin apocarotenoids in potato group phureja. *Engineering Reports.* 2024;e12997. doi: 10.1002/eng2.12997